Qeios

Effects of sediment disturbance by the heart urchin *Echinocardium cordatum* on the sediment–seawater solute exchange: an exclusion experiment

Roen McLeod, Michelle Simone and Kay Vopel*

School of Science, Auckland University of Technology, Auckland, New Zealand

*Correspondence: Kay Vopel, kay.vopel@aut.ac.nz

Keywords: Bioturbation, sediment–water solute exchange, oxygen, nitrogen

Abstract

Spatangoid heart urchins are dominant bioturbators in marine soft-sediment ecosystems worldwide. Their repeated sediment reworking prevents biogeochemical sediment stratification and colonisation by other species, with implications for sedimentary reaction processes that affect the local sediment–seawater solute exchange. Here, we used a simple exclusion experiment to investigate how a subtidal *Echinocardium cordatum* population (18.2 ± 6.7 individuals m^{-2}), foraging at an individual speed of ~45 cm per day affects the sediment–seawater solute exchange. To do so, we removed all heart urchins from eight one-meter-diameter areas of the 10-m deep seafloor of Man O'War Bay, Hauraki Gulf, New Zealand, and prevented recolonisation and hence sediment reworking for 56 days. Subsequently, we measured the sediment–seawater exchange of O_2, NO_3^-, NO_2^-, NH_4^+, and N_2 both within and outside the exclusion areas, under light or dark conditions, and found no difference. The absence of a legacy effect of foraging *E. cordatum* after their removal suggests that, at least in this habitat, their influence on the sediment–seawater solute exchange may be limited to sediment being displaced in the immediate surrounding of the urchin. This unexpected result underlines the importance of evaluating the influence of bioturbators on the sediment–seawater solute exchange in the context of local environmental conditions, animal behaviour, and population characteristics.

https://doi.org/10.32388/N7287X.3

Introduction

Macrofaunal bioturbation profoundly influences the mineralisation of carbon in seafloor sediment by displacing particles and solutes (Aller and Aller, 1998; Banta et al., 1999; Solan and Wingham, 2005; Kristensen et al., 2012). Persistent sediment disturbances by, for example, bottom trawling or deposition of organic fish farm waste, can alter the composition of the resident macrofaunal assemblage and therefore affect carbon remineralisation rates and the associated sediment–seawater exchange of dissolved carbon and nitrogen. Because this exchange links seafloor with pelagic ecosystem functions, changes in sediment bioturbation can have far-reaching consequences for coastal primary and secondary production (Forster et al., 1995; Lohrer et al., 2004; Volkenborn et al., 2007).

Heart urchins of the genus *Echinocardium* Gray, 1825 have a disproportionally large influence on sedimentary transport and reaction processes (Osinga et al., 1997; Lohrer et al., 2004, 2005, 2015). They are globally widespread through soft sediment environments, inhabiting intertidal mud or sand flats to abyssal plains, and can form up to 60% of the macrobenthic biomass in some ecosystems (Nakamura, 2001; De Ridder & Saucède, 2020). Functioning as key bioturbators, they alter the physical and biological structure of their surrounding sediment both directly, by mixing sediment particles and porewater (Lohrer et al., 2004, 2005; Kristensen et al., 2012), and indirectly, by suppressing the presence of tube building polychaetes and small bivalve species (authors unpublished observation).

One well-studied species of the genus *Echinocardium*, *E. cordatum* (Pennant, 1777), forages by burying itself at depths of up to 20 cm in sandy sediment and up to 6 cm in muddy (silt and clay) cohesive sediment (Buchanan, 1966; Foster-Smith, 1978; De Ridder & Saucède, 2020). Once buried, *E. cordatum* ploughs the sediment horizontally at speeds ranging from 1–8 cm h^{-1} (Buchanan, 1966; Lohrer et al., 2005; Vopel et al., 2007), selectively consuming microalgae and organic detritus (Smith, 1980; Boon & Duineveld, 2012; De Ridder et al., 2020). When foraging, *E. cordatum* can displace and mix 60–150 times more sediment particles than the amount it ingests (Hollertz & Duchêne, 2001; Lohrer et al., 2005).

To meet its respiratory requirements while buried, *E. cordatum* maintains a current that irrigates the restructured sediment with oxygenated seawater, thereby enhancing the oxidation of reduced solutes and particulates, a process that would otherwise be

56 constrained by the slow molecular diffusion of oxygen through cohesive sediment. Using
57 dorsal spines and tube feet, the urchin constructs and sustains a vertical funnel, connecting
58 the ambulacrum with the sediment surface (Buchanan, 1966; Smith, 1980). The cilia of the
59 ambulacral groove move oxygenated seawater down this funnel, facilitating gas exchange
60 over respiratory tube feet (Buchanan, 1966; De Ridder & Saucède, 2020). To prevent
61 suffocation due to the collapse of the respiratory funnel, the funnel-building tube feet
62 excrete and apply mucus to the wall of the funnel (Kanazawa, 1995; De Ridder & Saucède,
63 2020). Once the urchin has abandoned the funnel, microbial activity degrades this mucus,
64 causing the funnel to eventually collapse (Foster-Smith, 1978). Individuals dwelling in
65 shallow cohesive sediment often maintain a second, larger funnel that connects the
66 sediment surface in front of the urchin with the urchin's mouth (Vopel et al. 2007).
67 Furthermore, subanal spines and tube feet construct and sustain a sanitary drain, extending
68 laterally behind the urchin to accommodate excrements (De Ridder & Saucède, 2020).

69 The displacement of particles and porewater by *E. cordatum* may create effects that last
70 beyond the duration of the displacement event. For example, the tracks of *E. cordatum*
71 contribute to the small-scale roughness of the sediment surface, potentially influencing the
72 solute transport across the sediment–seawater interface (Buchanan, 1966. Vopel et al.
73 2007). Furthermore, particle mixing can stimulate sedimentary remineralisation and
74 oxidation processes by, respectively, introducing fresh organic matter into subsurface
75 sediment layers either in the form of excrements or by displacement from the surface, and
76 displacing reduced particles at depth to the surface, where they are exposed to oxygenated
77 seawater (Aller, 1982; Glud, 2008; Lohrer et al., 2004; Vopel et al., 2007, Braeckman et al.
78 2010). These effects can collectively enhance the remineralisation of labile and refractory
79 organic carbon, potentially altering the rates of the sediment–seawater exchange of
80 dissolved carbon and nitrogen.

81 Here, we asked if the previously demonstrated influence of moving *E. cordatum* on
82 sedimentary solute transport and reaction processes extends beyond the sediment
83 immediately next to the urchin. In other words, we asked if moving *E. cordatum* cause a
84 'legacy effect' that sustains a sediment–seawater solute exchange different from the
85 exchange across a similar but never disturbed sediment? If so, then removing *E. cordatum*
86 from the seafloor ecosystem should result in measurable difference between the solute

exchange across the now undisturbed surface sediment and the surface of the repeatedly reworked sediment.

We experimentally tested this prediction by removing urchins from eight plots of the 10-m deep seafloor of Man O'War Bay, Hauraki Gulf, New Zealand, and then preventing recolonisation and thus sediment reworking for about two months. Following this manipulation, we measured the sediment–seawater exchange of O_2, NO_3^-, NO_2^-, NH_4^+, and N_2 within and outside the exclusion areas. Because this exchange may be influenced by the activity of benthic algae and cyanobacteria, we conducted these measurements under conditions of light and darkness.

Methods and Materials

Study site

Man O'War Bay is situated on the east coast of Waiheke Island in the Hauraki Gulf, New Zealand (S 36° 47' 38", E 175° 10' 14", Fig. 1). The Hauraki Gulf covers nearly 4,000 km^2, with water depths up to 50 m and provides sheltered conditions that facilitate particle settling. The sediment in Man O'War Bay, which consists of terrigenous silt and clay with a small proportion of sand, is iron-rich, resulting in a dark grey-to-black subsurface layer due to an abundance of iron sulphides. Organic matter accounts for >6 % of the sediment dry weight, but the pore water of the top 20 cm of the sediment remains free of dissolved sulphides (Wilson & Vopel 2012). In May 2022, the salinity and temperature of the bottom seawater in Man O'War Bay were 34.5 and ~15 °C, respectively.

The seafloor at our 10-m deep site in Man O'War Bay is devoid of macroalgae and sessile epifauna, with golden-brown diatom patches that accentuate the centimetre-scale surface topography shaped by two bioturbators: a burrowing mud shrimp of the genus *Upogebia*, and the ploughing heart urchin *Echinocardium cordatum* (Fig. 2A). Other macroinfauna consists of small polychaetes (*Prionospio*, *Sthenelais,* and *Cossura*), an amphipod species (*Paraphoxus*), and a bivalve species (*Theora lubrica*) (Wong & O'Shea 2010).

To describe the resident population of *E. cordatum*, a seafloor survey was conducted two weeks before the exclusion experiment. SCUBA divers used a GoPro Hero 4 camera to capture a still images of a 0.5 × 0.5-meter quadrate placed on the surface of the seafloor at 40 locations randomly distributed within a 1260 m^2 area. At 10 locations, time-lapse

photography was used to estimate the speed at which individuals ploughed the sediment. The frame that held the underwater camera (Fig. 2A) was positioned within the camera's field of view, providing a reference for measuring distance.

Experimental procedures

On 3 May 2022, two SCUBA divers buried nine plastic rings (1 m diameter, 28 cm wide) within a ~700 m^2 circular area. The placement of each ring was carried out with a 30-m guide rope anchored in the sediment and nine pre-determined compass/distance coordinates (i.e., 0–360 degrees, 1–30 m away from the anchor). The divers pushed each ring ~25 cm deep into the sediment, leaving about 3 cm exposed above the sediment surface. Subsequently, they carefully removed all urchins (10–20 individuals per ring) from the area within the rings. The rings remained free of *E. cordatum* and in place for 56 days, effectively isolating the enclosed sediment from further sediment restructuring by the urchins.

On 27 June 2022, the divers returned to collect one intact sediment core from within (Treatment) and outside (Control) each of nine rings, at least 20 cm away from the edge of a ring, avoiding the sediment around openings of shrimp burrows shown in Figure 2A. To do so, they placed an acrylic tube (height: 300 mm, internal diameter: 90 mm) perpendicular to the seafloor and pushed 200 mm of the tube into the sediment until two-thirds were filled. They then inserted a lid with an open valve into the protruding end of the tube. This was done slowly, to avoid creating pressure inside the tube that would otherwise resuspend the silt sediment. Following this, the divers inserted a lid in the buried end of the tube pushing the sediment core inside the tube upwards by about one centimetre. They then closed the valve in the top lid and lifted the core out of the sediment. The sediment cores were stored upright in two large 50 L boxes containing ice, and transported to the laboratory within two hours.

Laboratory setup

In the laboratory, we removed the top lids of the acrylic tubes, and then submerged the sediment cores in the recirculating seawater (salinity = 34.5) of two 450-L holding tanks for a 3-day acclimatisation. A third and identical tank (measurement tank) was set up to which

sets of four or five cores were transferred for sediment–seawater solute flux measurements (see below).

Each tank was fitted with a pump (3260, Eheim) that moved ~9 L seawater per minute through a chiller unit (HC Chiller 300A, Hailea) and a UV steriliser (Pond One UV-C 9W, ClearTec) to a 200 L header tank from which the seawater returned to the tank by gravity. The chiller maintained the seawater temperature close to the in-situ seawater temperature (15 ± 0.5 °C). An additional pump pushed seawater through a UV particle filter (Aqua One Ocellaris 1400 UVC). A wave maker (SW, Jebao) attached to the inner wall of each tank, along with two jets of returning seawater from the UV particle filter and the header tank, ensured that advection was sufficient to prevent the seawater overlying the submerged sediment cores from becoming stagnant. Each tank had a Kessil A160WE Tuna Blue LED mounted above it, gradually increasing the intensity of photosynthetically active radiation (PAR) from 06:00 h to a midday maximum of ~120 µmol quanta m^{-2} s^{-1} and then gradually decreased this intensity until 18:00 h, when the LED was turned off. To account for evaporation, we monitored and adjusted the salinity of tank water each morning using reverse osmosis water.

Solute flux measurements

We transferred four or five cores at a time from the holding tanks into the measurement tank to determine the sediment–seawater solute flux under conditions of light and darkness. The light and dark solute flux was derived from the difference in the solute concentration in seawater collected ~10 mm above the sediment surface before and after a 4-h incubation period. This seawater was withdrawn slowly, using a tube connected to a syringe, avoiding particle resuspension. During the 4-h incubation period, the acrylic tube holding the sediment core and its overlying seawater was closed with a valved O-ring sealed lid. A peristaltic pump recirculated the enclosed seawater through Teflon tubes at a flow rate of 135 mL min^{-1} to prevent stagnation. The seawater O_2 concentration was measured at the beginning and the end of each incubation with a dipping probe (DP-PSt3, Presens GmbH) connected to a portable fibre optic oxygen meter (Microx 4, Presens GmbH). The O_2 concentration in the enclosed seawater never decreased below 86% saturation.

Sample analyses

For analyses of nitrite-N, nitrate+nitrite-N, and ammonia-N we collected, filtered (Sartorius CA 0.45 μm filter), and froze 10 mL of the seawater from each core, at the beginning and the end of each incubation. These samples were kept frozen until analyses. Seawater aliquots collected for N_2 analyses (2 × 12 mL exetainers) were poisoned with 0.01 mL of a saturated mercuric chloride solution. Following the seawater sampling, we decanted the seawater above the sediment cores, extruded the cores, and extracted the top 2 cm of sediment for granulometric analyses.

We determined the sediment granulometric indices by laser particle size analyses (Mastersizer 2000, Malvern Instruments Ltd.) of 10 homogenised samples, one taken from the top 2 cm of each of 5 Control and 5 Treatment cores. The sediment water content was determined as the loss of weight after 24 h drying at 90 °C. The seawater N_2 content was measured with a Pfeiffer Prismaplus QME mass spectrometer and a Bay Instruments S-25-75D membrane inlet, and the seawater concentrations of nitrite-N, nitrate+nitrite-N, and ammonia-N were determined with an Astoria Pacific 2 micro-segmented flow analyser (https://astoria-pacific.com/) following the Astoria protocols A182-A00 (range: 0.02–2.0 μmol L^{-1}), A177-A00 (range: 0.05–7.5 μmol L^{-1}) and A027-A00 (range: 0.05–5 μmol L^{-1}) for operating their respective individual nutrient channels (see also Rho et al. 2015).

Solute flux estimates

We determined the sediment–seawater solute flux (μmol m^{-2} h^{-1}) multiplying the start–end difference in solute concentrations (μmol L^{-1}) by the volume of enclosed seawater (L), and dividing this by the surface area of the sediment core (m^2) and the duration of the incubation (h). Because previous measurements revealed that the consumption/production of solutes in the seawater itself is negligible, this was not considered in our flux calculation. Note that a positive flux indicates sediment consumption whilst a negative flux is interpreted as solute release from the sediment.

Statistical Analysis

All statistical data analyses were completed with R-4.4.0 (R Core Team, 2022). For each solute we used Shapiro-Wilks test to confirm a normal distribution of the continuous variable. We then performed a two-way analysis of variance (ANOVA) investigating the

effects of light (light versus dark conditions), experimental treatment (cores from within the exclusion rings versus cores from outside the rings), and the interaction between these discrete predictors, on the direction and magnitude of each solute flux. Visual analysis of the diagnostic plots for each of the five solutes confirmed that they met the assumptions of an ANOVA, including homogeneity of variance. When a significant result was found (alpha threshold = 0.05), we followed with post-hoc TukeyHSD analyses to further investigate significant individual effects.

Results

Habitat

The sediment in the sheltered Man O'War Bay consisted of ~74% silt, 17% sand, and ~9% clay. The laser particle size analyses returned the following granulometric indices: Median = 30 µm (silt), Lower Quartile Q1 = 63 µm, Upper Quartile Q3 = 10 µm, Inclusive Sorting Coefficient QD1 = 1.95 (poorly sorted), and Inclusive Graphic Skewness Sk_1 = 0.07. The water content of the sediment decreased from 75% in the top 2 cm to 65% at 9 cm depth.

Analyses of 100 photographs of the sediment surface revealed ~18.2 $\pm$ 6.7 (mean $\pm$ SD, n = 100) *Echinocardium cordatum* individuals per square meter. Time-lapse videos showed that urchins moved at ~45 $\pm$ 12 cm per day (mean $\pm$ SD, n = 6).

Experimental control

The sediment outside the exclusion rings, between foraging *E. cordatum*, and away from the immediate surrounding of the urchin, consumed O_2 at similar rates under conditions of darkness and light (Table 1, Figs 2B, 3). In light, this sediment took up on average ~39% more N_2 from the overlying seawater then under conditions of darkness (Table 1, Figs 2B, 3). The average sediment–seawater fluxes of nitrate and nitrite were an order of magnitude lower than that of N_2; on average nitrate was released (negative flux in Table 1, Figs 2B, 3) while nitrite was taken up by the sediment, at similar rates under conditions of light and darkness (Figs 2B, 3).

The flux of ammonium in light differed significantly from that measured in darkness ($p < 0.025$, Table 1, 2). In light, the sediment released ammonium into the overlying seawater

(negative flux in Table 1), while the average of fluxes measured in darkness indicated a small uptake (Table 1, Figs 2B, 3).

Sea urchin exclusion–experimental treatment

The solute fluxes (O_2, N_2, NO_3^-, NO_2^-, NH_4^+) across the surface of the sediment collected within the exclusion rings (Treatment) did not significantly differ from the fluxes measured across the surface of the sediment collected outside the exclusion rings (Control), under conditions of both light and darkness (Tables 1, 2, Fig. 3).

Discussion

We expected that the exchange of dissolved oxygen and nitrogen across the surface of the sediment that lies beyond the immediate surrounding of foraging *E. cordatum* individuals would reflect a history of repeated reworking, so that after a 56-day cessation of this reworking the solute fluxes measured inside (Treatment) and outside (Control) the urchin exclusion rings would differ in their magnitude and/or direction. Our measurements, however, did not reveal any statistically significant differences between Treatment and Control. We considered the potential influence of *E. cordatum* on sedimentary solute reaction processes; repeated particle mixing and porewater oxygenation should have altered remineralisation rates and thus modified the associated sediment–seawater solute exchange. Apparently, the rate at which the sediment was mixed and oxygenated by the resident *E. cordatum* population did not cause the expected influence, so that the removal of urchins didn't make a difference.

Besides the potential direct effects of sediment mixing on microbial reaction processes, we expected indirect effects, which can result from the influence of *E. cordatum* on cohabiting biota, most importantly, benthic microphytes. Photosynthesis of microphytes can cause dark/light differences in the total sediment–seawater O_2 exchange as measured by core incubations, and an influence of *E. cordatum* on the abundance and activity of microphytes would then be evident from either an increase or decrease of these differences. Our sediment core incubations revealed, however, that the Control removed as much O_2 from the bottom seawater in darkness than it did in light (Table 1). Assuming that the O_2 demand of the sediment in light did not differ from that in darkness, this suggests that benthic photosynthetic O_2 production must have been negligible. If this was the result of heart

urchin predation limiting the growth of microphytes, then we would expect algae growth and photosynthesis to increase following the exclusion of the heart urchins. However, there was no evidence of such increase; apparently, benthic primary production in the Control sediment was not limited by predation, so that removal of predation as a potential factor made no difference.

Other studies reported a positive correlation between the abundance of *E. cordatum* (consuming microphytobenthos) and the chlorophyll-*a* content of its surrounding sediment (Needham et al., 2011; Lohrer et al., 2004, 2005, 2015). In habitats where photosynthetically active radiation (PAR) is not limiting microphytobenthic production, this may follow from a stimulation of bacterial mineralisation processes, increasing the porewater concentrations of inorganic nitrogen, so that algal growth outweighs consumption. Such gardening effect will be subject to seasonal variations in environmental conditions and heart urchin abundance and activity. Lower PAR and temperature in winter, for example, can hamper benthic primary production and slow urchin movement, respectively (Seike et al., 2022). A repeat of our study in November/December may reveal if the influence of *E. cordatum* on the sediment–seawater solute exchange at our site in fact depends on seasonal changes in conditions for growth and production of microphytes or if what we have observed in May/June generally applies throughout the year.

Interestingly, both sediments, Control and Treatment, served as a sink for N_2. Others have reported nitrogen fixation in ammonium-rich sediments, like those found in seagrass beds (Aoki & McGlathery, 2019) or subtidal coastal sediments (Fulweiler et al., 2007, Newell et al., 2016), and such fixation may be limited to microenvironments in which nitrogen becomes limiting (Whiting et al. 1986). As Bertics et al. (2013) pointed out, however, sediments rich in organic matter and reduced substrates provide an unusual conundrum for anaerobic organisms—the excess electrons can damage cells and there is a need to regenerate electron carriers. Nitrogen fixation may be a mechanism for dissipating reducing power and maintaining an ideal intracellular redox state (Joshi & Tabita, 1996, Bombar et al., 2016), so that nitrogen fixation is observed despite high ammonium concentrations.

The significant light–dark difference in the ammonium exchange of the Control sediment—a small uptake under conditions of darkness, but release in light—suggests an influence of photosynthesis on nitrogen cycling. This is contrast to the interpretation of our light/dark O_2

exchange data (negligible benthic photosynthesis, see above), and raises the question if our assumption of similar sediment O_2 demand in light and darkness was valid. If the sediment O_2 demand in light was greater than in darkness, then benthic photosynthesis may have played a role without leaving a measurable signature in the total sediment–seawater O_2 exchange. Assuming that the ammonium and N_2 concentrations in the sediment overlying seawater remained stable and independent of light, then the difference in the derived sediment–seawater flux must have resulted from changes in the sediment porewater solute concentrations. Phototrophs assimilating ammonium in darkness, but not in light, would then cause a light/darkness difference in the sediment–seawater ammonium exchange. Similarly, if more porewater N_2 was to be consumed by diazotrophs in light than in darkness (energy limited N_2 fixation; Stal, 2015), then this would explain why the sediment uptake was greater in light than in darkness. Alternatively, a production of N_2 via anammox in darkness would increase the porewater N_2 concentration and so lower the rate at which the sediment removes N_2 from the bottom seawater. Because this process also lowers the porewater ammonium concentration, it can explain both observations, a lower release or even uptake of ammonium, and lower uptake of N_2 under conditions of darkness.

In conclusion, although foraging *E. cordatum* enhance the sediment–seawater solute exchange where and when they displace sediment particles, this effect does not necessarily outlast the disturbance event. At our subtidal site, at least in May/June, removal of the heart urchins did not alter the solute exchange across the surface of the sediment area that is not actively disturbed. This underlines the importance of evaluating the influence of bioturbators on ecosystem processes in the context of local environmental conditions, seasonal changes in these conditions and biological activity, urchin behaviour, and population characteristics.

Acknowledgments

Evan Brown assisted in the field. K.V. designed the experiment, R.M. and M.S. with the assistance of Mohammad H. A. Usmani completed the laboratory sediment incubations. M.S. measured the inorganic nitrogen content of seawater samples, and R.M. and K.V. analysed the data and wrote the manuscript.

References

Aller, R. C. (1982). The Effects of macrobenthos on chemical properties of marine sediment and overlying water. In P. L. McCall & M. J. S. Tevesz (Eds.), Animal-Sediment Relations (Vol. 100, pp. 53–102). Springer US. https://doi.org/10.1007/978-1-4757-1317-6_2

Aller, R. C., & Aller, J. Y. (1998). The effect of biogenic irrigation intensity and solute exchange on diagenetic reaction rates in marine sediments. Journal of Marine Research, 56(4), 905–936. https://doi.org/10.1357/002224098321667413

Aoki, L., & McGlathery, K. (2019). High rates of N fixation in seagrass sediments measured via a direct 30N2 push-pull method. Marine Ecology Progress Series, 616, 1–11. https://doi.org/10.3354/meps12961

Banta, G., Holmer, M., Jensen, M., & Kristensen, E. (1999). Effects of two polychaete worms, *Nereis diversicolor* and *Arenicola marina*, on aerobic and anaerobic decomposition in a sandy marine sediment. Aquatic Microbial Ecology, 19, 189–204. https://doi.org/10.3354/ame019189

Bertics, V. J., Löscher, C. R., Salonen, I., Dale, A. W., Gier, J., Schmitz, R. A., & Treude, T. (2013). Occurrence of benthic microbial nitrogen fixation coupled to sulfate reduction in the seasonally hypoxic Eckernförde Bay, Baltic Sea. Biogeosciences, 10(3), 1243–1258. https://doi.org/10.5194/bg-10-1243-2013

Bombar, D., Paerl, R. W., & Riemann, L. (2016). Marine non-cyanobacterial diazotrophs: Moving beyond molecular detection. Trends in Microbiology, 24(11), 916–927. https://doi.org/10.1016/j.tim.2016.07.002

Boon, A. R., & Duineveld, G. C. A. (2012). Phytopigments and fatty acids in the gut of the deposit-feeding heart urchin *Echinocardium cordatum* in the southern North Sea: Selective feeding and its contribution to the benthic carbon budget. Journal of Sea Research, 67(1), 77–84. https://doi.org/10.1016/j.seares.2011.10.004

Braeckman, U., Provoost, P., Gribsholt, B., Van Gansbeke, D., Middelburg, J.J., Soetaert, K., Vincx, M. and Vanaverbeke, J. (2010). Role of macrofauna functional traits and density in biogeochemical fluxes and bioturbation. Marine Ecology Progress Series, 399, 173–186.

Buchanan, J. B. (1966). The biology of *Echinocardium cordatum* [Echinodermata: Spatangoidea] from different habitats. Journal of the Marine Biological Association of the United Kingdom, 46(1), 97–114. https://doi.org/10.1017/S0025315400017574

De Ridder, C., Jangoux, M., & Impe, E. (2020). Food selection and absorption efficiency in the spatangoid echinoid, *Echinocardium cordatum* (Echinodermata). In B. F. Keegan & B. D. S. O'Connor (Eds.), Echinodermata (1st ed., pp. 245–251). CRC Press. https://doi.org/10.1201/9781003079224-48

De Ridder, C., & Saucède, T. (2020). *Echinocardium cordatum*. In Developments in Aquaculture and Fisheries Science (Vol. 43, pp. 337–357). Elsevier. https://doi.org/10.1016/B978-0-12-819570-3.00020-2

Forster, S., Graf, G., Kitlar, J., & Powilleit, M. (1995). Effects of bioturbation in oxic and hypoxic conditions: A microcosm experiment with a North Sea sediment community. Marine Ecology Progress Series, 116, 153–161. https://doi.org/10.3354/meps116153

Foster-Smith, R. L. (1978). An analysis of water flow in tube-living animals. Journal of Experimental Marine Biology and Ecology, 34(1), 73–95. https://doi.org/10.1016/0022-0981(78)90058-8

Fulweiler, R. W., Nixon, S. W., Buckley, B. A., & Granger, S. L. (2007). Reversal of the net dinitrogen gas flux in coastal marine sediments. Nature, 448(7150), 180–182. https://doi.org/10.1038/nature05963

Glud, R. N. (2008). Oxygen dynamics of marine sediments. Marine Biology Research, 4(4), 243–289. https://doi.org/10.1080/17451000801888726

Hollertz, K., & Duchêne, J. C. (2001). Burrowing behaviour and sediment reworking in the heart urchin *Brissopsis lyrifera* Forbes (Spatangoida). Marine Biology, 139(5), 951–957. https://doi.org/10.1007/s002270100629

Joshi, H. M., & Tabita, F. R. (1996). A global two component signal transduction system that integrates the control of photosynthesis, carbon dioxide assimilation, and nitrogen fixation. Proceedings of the National Academy of Sciences, 93(25), 14515–14520. https://doi.org/10.1073/pnas.93.25.14515

Kanazawa, K. (1995). How spatangoids produce their traces: Relationship between burrowing mechanism and trace structure. Lethaia, 28(3), 211–219. https://doi.org/10.1111/j.1502-3931.1995.tb01424.x

Kristensen, E., Penha-Lopes, G., Delefosse, M., Valdemarsen, T., Quintana, C., & Banta, G. (2012). What is bioturbation? The need for a precise definition for fauna in aquatic sciences. Marine Ecology Progress Series, 446, 285–302. https://doi.org/10.3354/meps09506

Lohrer, A. M., Thrush, S. F., & Gibbs, M. M. (2004). Bioturbators enhance ecosystem function through complex biogeochemical interactions. Nature, 431(7012), 1092–1095. https://doi.org/10.1038/nature03042

Lohrer, A. M., Thrush, S. F., Hewitt, J. E., & Kraan, C. (2015). The up-scaling of ecosystem functions in a heterogeneous world. Scientific Reports, 5(1), 10349. https://doi.org/10.1038/srep10349

Lohrer, A. M., Thrush, S. F., Hunt, L., Hancock, N., & Lundquist, C. (2005). Rapid reworking of subtidal sediments by burrowing spatangoid urchins. Journal of Experimental Marine Biology and Ecology, 321(2), 155–169. https://doi.org/10.1016/j.jembe.2005.02.002

Nakamura, Y. (2001). Autoecology of the heart urchin, *Echinocardium cordatum*, in the muddy sediment of the Seto Inland Sea, Japan. Journal of the Marine Biological Association of the United Kingdom, 81(2), 289–297. https://doi.org/10.1017/S0025315401003769

Nedwell, D. B., & Walker, T. R. (1995). Sediment-water fluxes of nutrients in an Antarctic coastal environment: Influence of bioturbation. Polar Biology, 15(1). https://doi.org/10.1007/BF00236125

Needham, H. R., Pilditch, C. A., Lohrer, A. M., & Thrush, S. F. (2011). Context-specific bioturbation mediates changes to ecosystem functioning. Ecosystems, 14(7), 1096–1109. https://doi.org/10.1007/s10021-011-9468-0

Newell, S. E., McCarthy, M. J., Gardner, W. S., & Fulweiler, R. W. (2016). Sediment nitrogen fixation: A call for re-evaluating coastal N budgets. Estuaries and Coasts, 39(6), 1626–1638. https://doi.org/10.1007/s12237-016-0116-y

Osinga, R., Kop, A. J., Malschaert, J. F. P., & Van Duyl, F. C. (1997). Effects of the sea urchin *Echinocardium cordatum* on bacterial production and carbon flow in experimental benthic systems under increasing organic loading. Journal of Sea Research, 37(1–2), 109–121. https://doi.org/10.1016/S1385-1101(97)00003-8

R Core Team. (2022). R: A language and environment for statistical computing. [Computer software]. R Foundation for Statistical Computing. https://www.R-project.org/

Rho, T, Coverly, S., Kim, E.-S., Kang, D.-J., Kahn, S.-H., Na, T.-H., Cho, S.-R., Lee, J.-M., Moon, C.-R. (2016) Practical considerations for the segmented-flow analysis of nitrate and ammonium in seawater and the avoidance of matrix effects. Ocean Science Journal, 50(4), 709–720. https://doi.org/10.1007/s12601-015-0064-7

Seike, K., Sassa, S., Shirai, K., & Kubota, K. (2022). Sediment hardness and water temperature affect the burrowing of *Echinocardium cordatum*: Implications for mass mortality during the 2011 earthquake–liquefaction–tsunami disaster. Estuarine, Coastal and Shelf Science, 267, 107763. https://doi.org/10.1016/j.ecss.2022.107763

Smith, A. B. (1980). The structure and arrangement of echinoid tubercles. Philosophical Transactions of the Royal Society of London. B, Biological Sciences, 289(1033), 1–54. https://doi.org/10.1098/rstb.1980.0026

Solan, M., & Wigham, B. D. (2005). Biogenic particle reworking and bacterial–invertebrate interactions in marine sediments. In E. Kristensen, R. R. Haese, & J. E. Kostka (Eds.), Coastal and Estuarine Studies (Vol. 60, pp. 105–124). American Geophysical Union. https://doi.org/10.1029/CE060p0105

Stal, L. J. (2015). Nitrogen Fixation in Cyanobacteria. In Wiley, Encyclopedia of Life Sciences (1st ed., pp. 1–9). Wiley. https://doi.org/10.1002/9780470015902.a0021159.pub2

Volkenborn, N., Hedtkamp, S. I. C., van Beusekom, J. E. E., & Reise, K. (2007). Effects of bioturbation and bioirrigation by lugworms (*Arenicola marina*) on physical and chemical sediment properties and implications for intertidal habitat succession. Estuarine, Coastal and Shelf Science, 74(1–2), 331–343. https://doi.org/10.1016/j.ecss.2007.05.001

Vopel, K., Vopel, A., Thistle, D., & Hancock, N. (2007). Effects of spatangoid heart urchins on O_2 supply into coastal sediment. Marine Ecology Progress Series, 333, 161–171. https://doi.org/10.3354/meps333161

Whiting, G. J., Gandy, E. L., & Yoch, D. C. (1986). Tight coupling of root-associated nitrogen fixation and plant photosynthesis in the salt marsh grass *Spartina alterniflora* and carbon dioxide enhancement of nitrogenase activity. Applied and Environmental Microbiology, 52(1), 108–113. https://doi.org/10.1128/aem.52.1.108-113.1986

Wilson, P. S., Vopel, K. (2012) Estimating the in situ distribution of acid volatile sulfides from sediment profile images. Limnology and Oceanography: Methods, 10(12), 1070–1077. https://doi.org/10.4319/lom.2012.10.1070

449 Wong, K. C., & O'Shea, S. (2010). Sediment macrobenthos off eastern Waiheke Island,
450 Hauraki Gulf, New Zealand. New Zealand Journal of Marine and Freshwater Research,
451 44(3), 149–165. https://doi.org/10.1080/00288330.2010.498088
452

Figure captions

Figure 1. Map depicting the North Island of New Zealand and the study site (insert, yellow marker) in Man O'War Bay, at the East shore of Waiheke Island, Hauraki Gulf, New Zealand (S 36° 47' 38", E 175° 10' 14").

Figure 2. (A) Sediment surface at Man O'War Bay, Hauraki Gulf, New Zealand, showing tracks (tr) made by the heart urchin *Echinocardium cordatum*. Orange arrows indicate the direction of the heart urchin's movement. Black arrows indicate the respiratory (rf) and feeding (ff) funnels. Larger holes are the openings of shrimp burrows, presumably made by *Upogebia* sp. Darker areas lining the tracks are diatoms. (B) Schematic illustrating the direction and magnitude of the sediment–seawater solute flux under conditions of light (light grey arrows) and darkness (dark grey arrows). The horizontal line indicates the sediment surface.

Figure 3. Sediment–seawater flux (µmol m^{-2} h^{-1}, n = 9) of ammonium (NH_4^+), nitrite (NO_2^-), nitrate (NO_3^-), nitrogen gas (N_2), and oxygen (O_2) in darkness (closed symbols) and light (open symbols), derived from laboratory incubations of sediment collected in Man O' War Bay, Hauraki Gulf, New Zealand outside (Control) and inside (Treatment) sea urchin exclusion rings after 56 days. A positive flux indicates sediment solute uptake. Horizontal bars are means, the asterisk indicates a significant difference, and the hash sign marks two groups from each of which one outlier has been removed (n = 8).

473 Table 1. Mean sediment–seawater flux (µmol m^{-2} h^{-1}, Mean ± C.I., n = 9) of ammonium
474 (NH_4^+), nitrite (NO_2^-), nitrate (NO_3^-), nitrogen gas (N_2), and oxygen (O_2) in darkness and light,
475 derived from laboratory incubations of sediment collected in Man O' War Bay, Hauraki Gulf,
476 New Zealand outside (Control) and inside (Treatment) sea urchin exclusion rings after 56
477 days. A positive flux indicates sediment solute uptake. Number in parenthesis, n; hash sign,
478 one outlier removed.

479

	Control		Treatment	
	Darkness	Light	Darkness	Light
N_2	121.4 ± 28.6 (9)	169.2 ± 35.1 (9)	93.7 ± 24.5 (9)	141.3 ± 30.4 (8)[#]
O_2	149.6 ± 22.8 (9)	140.4 ± 23.8 (8)[#]	148.2 ± 29.0 (9)	137.6 ± 45.3 (9)
NO_2^-	13.3 ± 18.9 (9)	8.1 ± 25.9 (9)	5.8 ± 7.7 (9)	7.6 ± 16.2 (9)
NO_3^-	-22.8 ± 20.8 (9)	-22.9 ± 26.5 (9)	-18.2 ± 9.1 (9)	-22.4 ± 19.3 (9)
NH_4^+	2.5 ± 29.0 (9)	-49.7 ± 13.7 (9)	-6.5 ± 11.3 (9)	-30.4 ± 11.8 (9)

480

Table 2. Two-way ANOVA and TukeyHSD (df, Mean Sum of Squares, F values, adjusted P Values, C.I. 95%) of solute flux across the surface of sediment cores as a function of the presence (Control) or absence (Treatment) of *Echinocardium cordatum*, the measurement light regime (light/dark), and their interaction.

Solute	df	Mean SS	F value	P value	TukeyHSD
N_2					
Urchin presence	1	7449	3.658	0.055	
Light regime	1	19835	9.741	<0.004	CL:TD < 0.00066
Interaction	1	0	0	0.996	
O_2					
Urchin presence	1	560	0.164	0.458	
Light regime	1	3707	1.087	0.247	
Interaction	1	395	0.116	0.429	
NO_2^-					
Urchin presence	1	142	0.180	0.674	
Light regime	1	26	0.033	0.857	
Interaction	1	108	0.136	0.714	
NO_3^-					
Urchin presence	1	59	0.063	0.803	
Light regime	1	39	0.042	0.839	
Interaction	1	37	0.040	0.843	
NH_4^+					
Urchin presence	1	240	0.317	0.577	
Light regime	1	13026	17.171	<0.001	CL:CD < 0.025; CL:TD < 0.019
Interaction	1	1804	2.378	0.133	

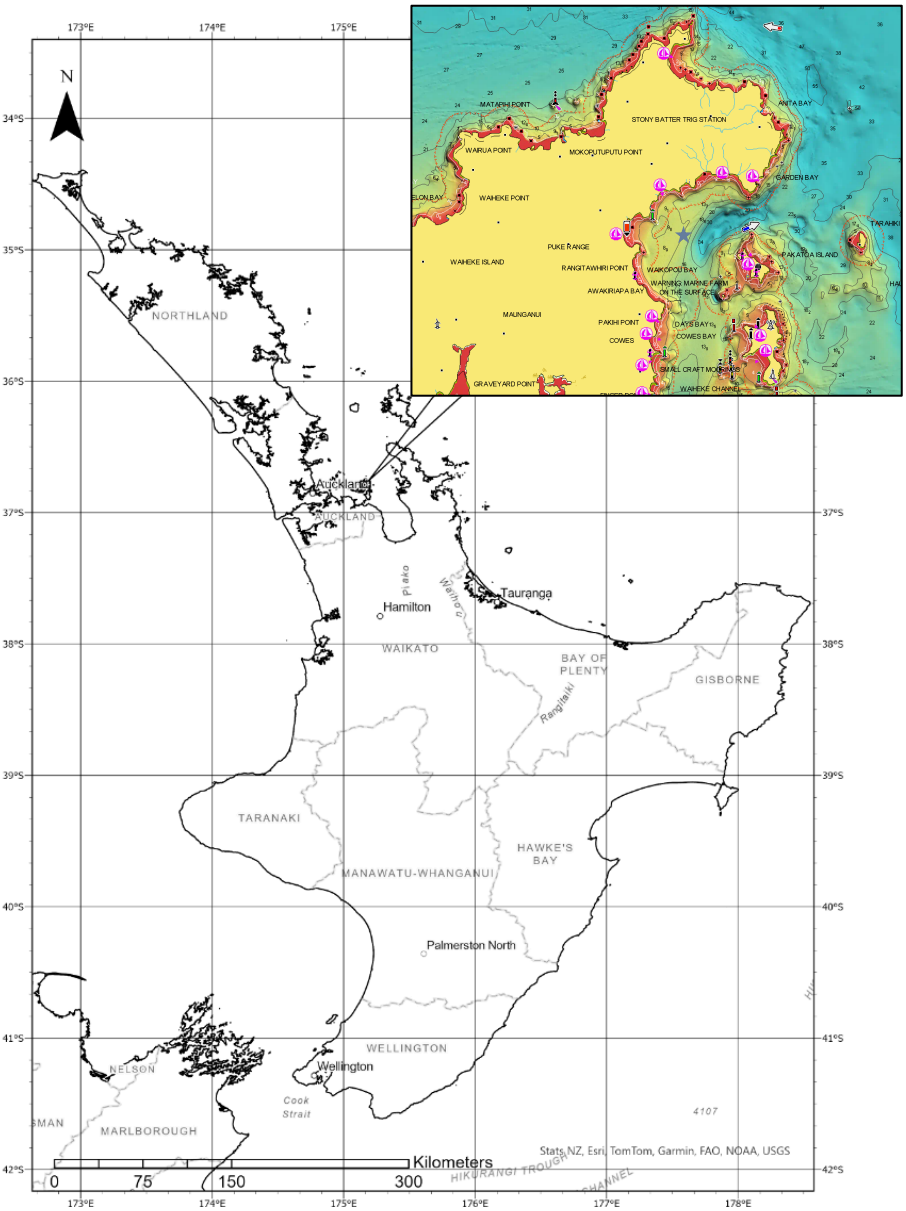

488

489 Figure 1.

490

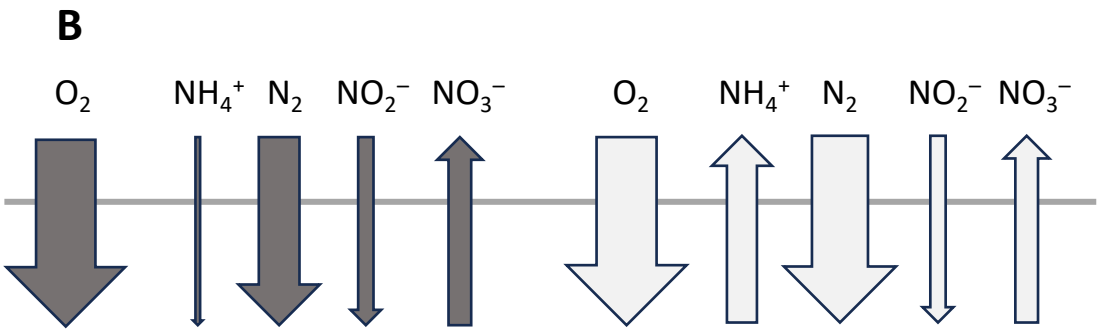

491

492 Figure 2

493

494

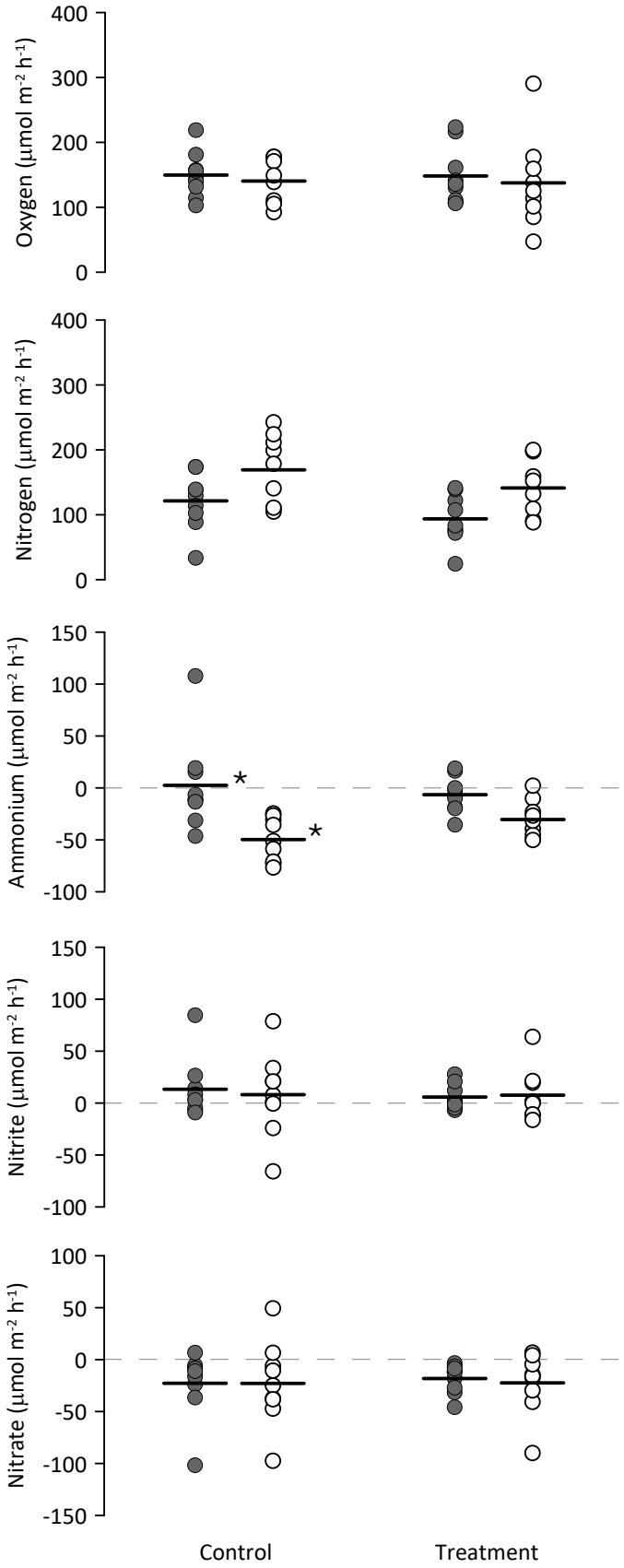

495

496 Figure 3.